Effect of Streamflow Component Structure on Characterizing Storage–Discharge Dynamics in an Analytical Probabilistic Streamflow Model

Chia-Chi Huang, Hsin-Fu Yeh and Ya-Sin Yang
Department of Resources Engineering, National Cheng Kung University, Tainan 701401, Taiwan (chi840715@gmail.com)

EGU24-6990

Sharing not permitted

I. Summary

- The differences in recession parameters and streamflow complexity between catchments highlight their relationships with catchment characteristics.
- Modelled recession parameters from FDCs demonstrated the storage–discharge mechanisms associated with streamflow component structures.
- The conformity of streamflow component structures to the model's basic assumptions can be evaluated through the model performance.

II. Introduction

- Streamflow represents the hydrological output behavior of the catchment system and can elucidate the physical processes of other hydrological variables.
- The difference of streamflow contributions between catchment can be revealed by separating the streamflow into numbers of component (Stoelzle et al., 2020).
- Capturing the characteristic timescale for streamflow events will help to construct an unique model structures of a catchment (Leong and Yokoo, 2022).

III. Study Area

This study selected 8 streamflow gauging stations in the Chuoshui River Basin. The daily gridded rainfall P datasets from the Taiwan Climate Change Projection Information and Adaptation Knowledge Platform (TCCIP) were used.

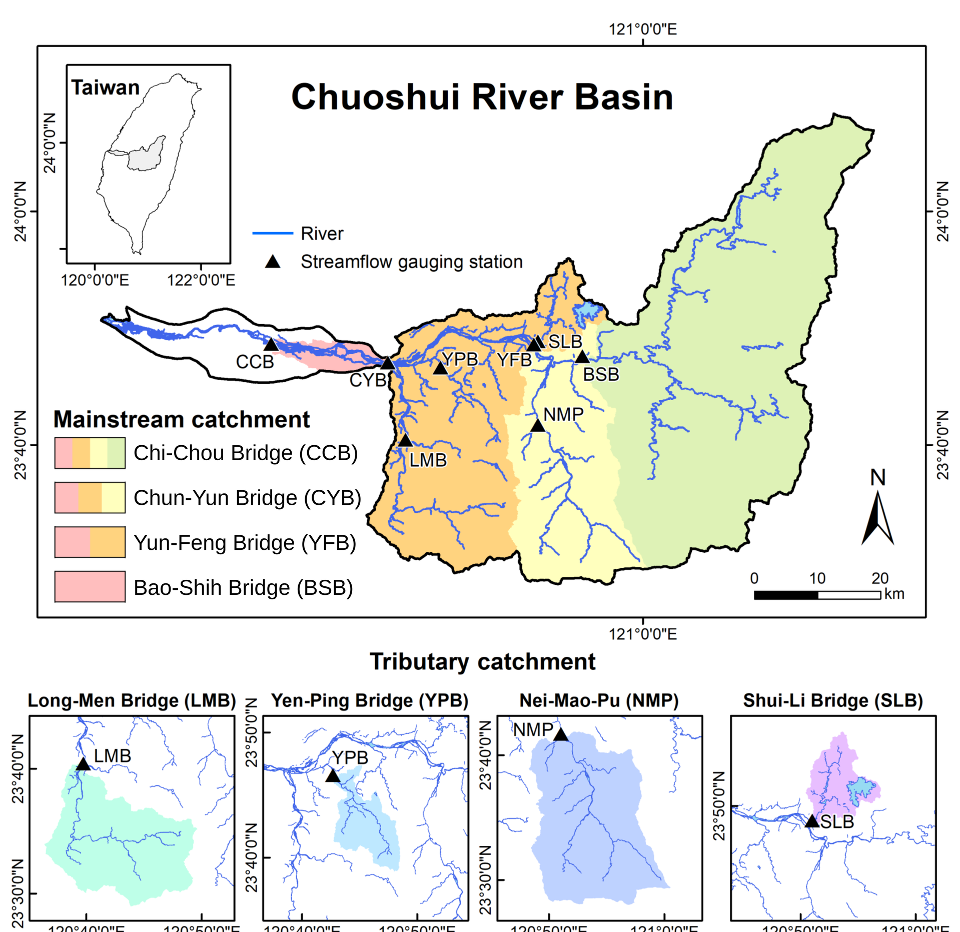

Fig. 1 Selected stations and catchments in the Chuoshui River Basin. (Huang and Yeh, 2022)

Table 1. Selected gauging stations (data period larger than 10 years) and catchment characteristics in the Chuoshui River Basin.

Station	Area (km²)	Elevation (m)	Slope (%)
CCB	2974.7	1516.5	72.1
CYB	2906.3	1547.0	73.6
YFB	2098.9	1838.5	81.9
BSB	1542.4	1956.1	83.7
LMB	360.0	1137.9	68.4
YPB	86.5	815.6	53.9
NMP	367.4	1716.1	80.9
SLB	80.2	699.2	49.0

References

- Botter, G., Porporato, A., Rodriguez-Iturbe, I., and Rinaldo, A. (2009). Nonlinear storage-discharge relations and catchment streamflow regimes. Water resources research, 45(10), W10427.
- Hino, M., and Hasebe, M. (1984). Identification and prediction of nonlinear hydrologic systems by the filter-separation autoregressive (AR) method: Extension to hourly hydrologic data. *Journal of Hydrology, 68*(1), 181-210.
- Huang, C. C., and Yeh, H. F. (2022). Evaluation of seasonal catchment dynamic storage components using an analytical streamflow duration curve model. *Sustainable Environment Research, 32*(1), 49.
- Stoelzle, M., Schuetz, T., Weiler, M., Stahl, K., and Tallaksen, L. M. (2020). Beyond binary baseflow separation: a delayed-flow index for multiple streamflow contributions. *Hydrology and Earth System Sciences, 24*(2), 849-867.
- Leong, C., and Yokoo, Y. (2022). A multiple hydrograph separation technique for identifying hydrological model structures and an interpretation of dominant process controls on flow duration curves. *Hydrological Processes, 36*(4), e14569.

IV. Methodology

4.1 Multiple hydrograph separation

Recession selection and fitting

- Continuous streamflow Q decay for at least 5 consecutive days
- the discharge from aquifer leads to an exponential baseflow recession:

$$Q(t) = a\,exp\left(-\frac{t}{K}\right)$$

a is intercept of Q; K is the recession index also known as drainage characteristics timescale

Determination of K for i-th streamflow component structures (K_i)

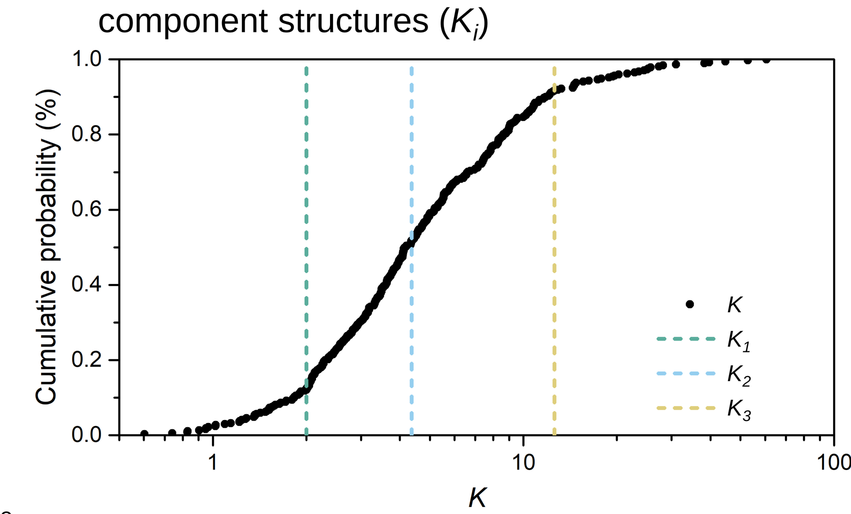

Fig. 2 Cumulative distribution function of K

Autoregressive numerical filter separation

The slow components Q_i are separated from observed streamflow Q using the filter which determines the cut-off frequency by the constant K (Hino and Hasebe, 1984)

$$Q_i(t) = \sum_{\tau=0}^{\tau_{max}} \omega_i(\tau)\cdot Q(t-\tau)$$

$$\omega(\tau) = \begin{cases} c_0\sqrt{\frac{c_1^2}{4}-c_0}\cdot\left[exp\left(-\frac{c_1\tau}{2}\right)\right]sinh\left(\sqrt{\frac{c_1^2}{4}-c_0\tau}\right), & \tau>0 \\ 0, & \tau\le 0 \end{cases}$$

τ is time axis; ω is the numerical filter; c_0 and c_1 are δ^2/K^2 and δ^2/K (δ is the damping factor)

This study repeated the separations to yield the slower component structure (Q_i)

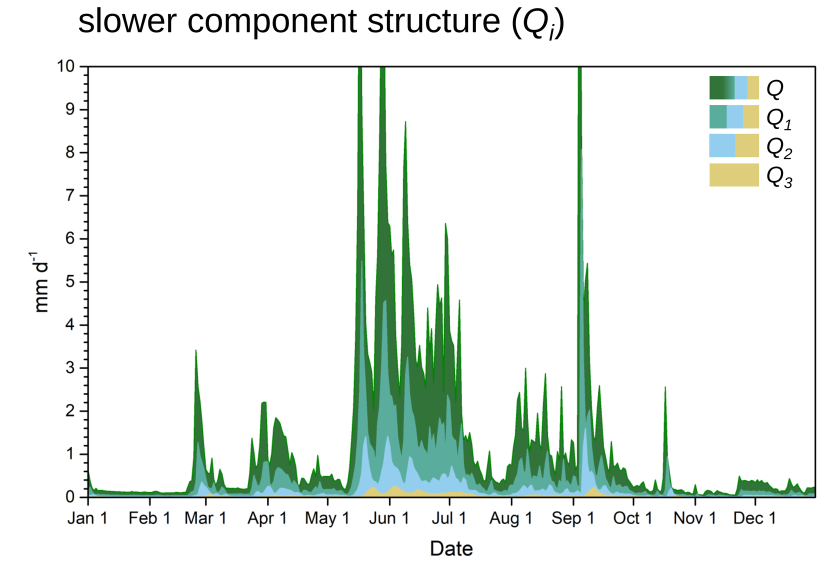

Fig. 3 Diagram of multiple hydrograph separation in CCB catchment

4.2 Flow duration curve (FDC) analytical model

It provides an estimation of recession parameters b and a ($-dQ/dt = aQ^b$) through all streamflow data Q rather than selected recession data. (Botter et al., 2009).

Rainfall Poisson process

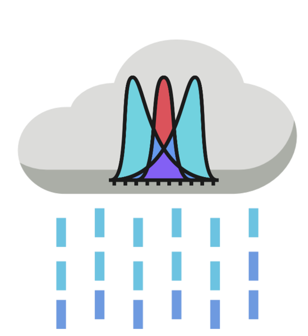

Model assumption

Groundwater discharge generates streamflow when a sequence of rainfall events increases soil moisture beyond retention capacity.

Stochastic distribution function of the daily streamflow:

$$p(Q, t\to\infty) = C\left\{\frac{1}{Q^b}exp\left[-\frac{Q^{2-b}}{P_e\cdot a(2-b)}+\frac{Q^{1-b}\lambda}{a(1-b)}\right]\right\}$$

C	a normalizing constant
P_e	the average effective rainfall
λ	the ratio of average streamflow to average effective rainfall

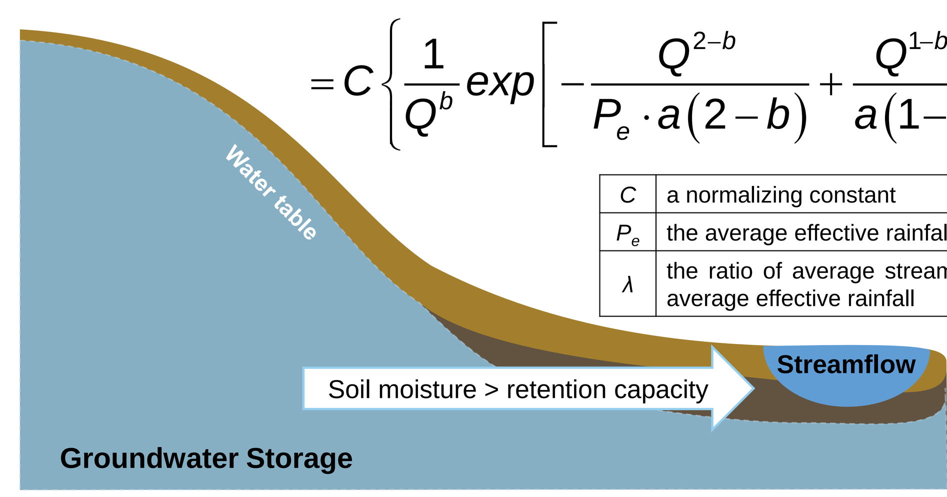

Maximum likelihood estimation

$$L(b,a) = \prod_{i=1}^{N} p(Q;b;a)$$

Cumulative Distribution Function (cdf)

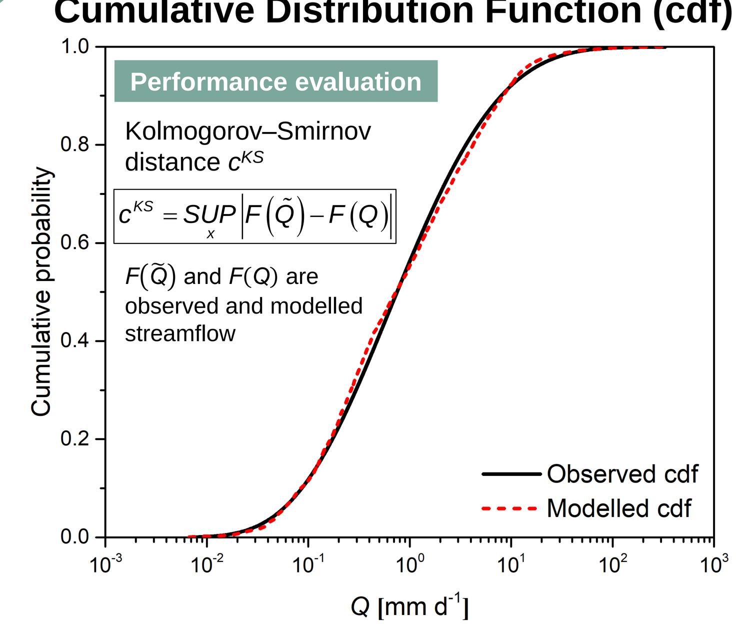

Fig. 4 Observed and modelled cdfs of CCB catchment

V. Results & Discussion

5.1 K values corresponding to i-th streamflow structure (K_i)

- The decline in K_2 values moving from upstream to downstream areas suggests the presence of geomorphological influences on dominant drainage dynamics.

Table 2. Determination of K_1, K_2, and K_3 in each catchment

K_i	CCB	CYB	YFB	BSB	LMB	YPB	NMP	SLB
K_1	2.00	1.62	3.69	4.04	2.18	1.8	6.00	2.21
K_2	4.36	5.46	14.78	16.71	9.66	5.62	20.03	6.58
K_3	12.58	17.44	70.13	58.52	50.35	21.95	78.79	15.29

5.2 FDCs and model performance

- Despite slight improvements in some catchments, it still reveals the importance of streamflow component structures in assessing the storage–discharge dynamics.

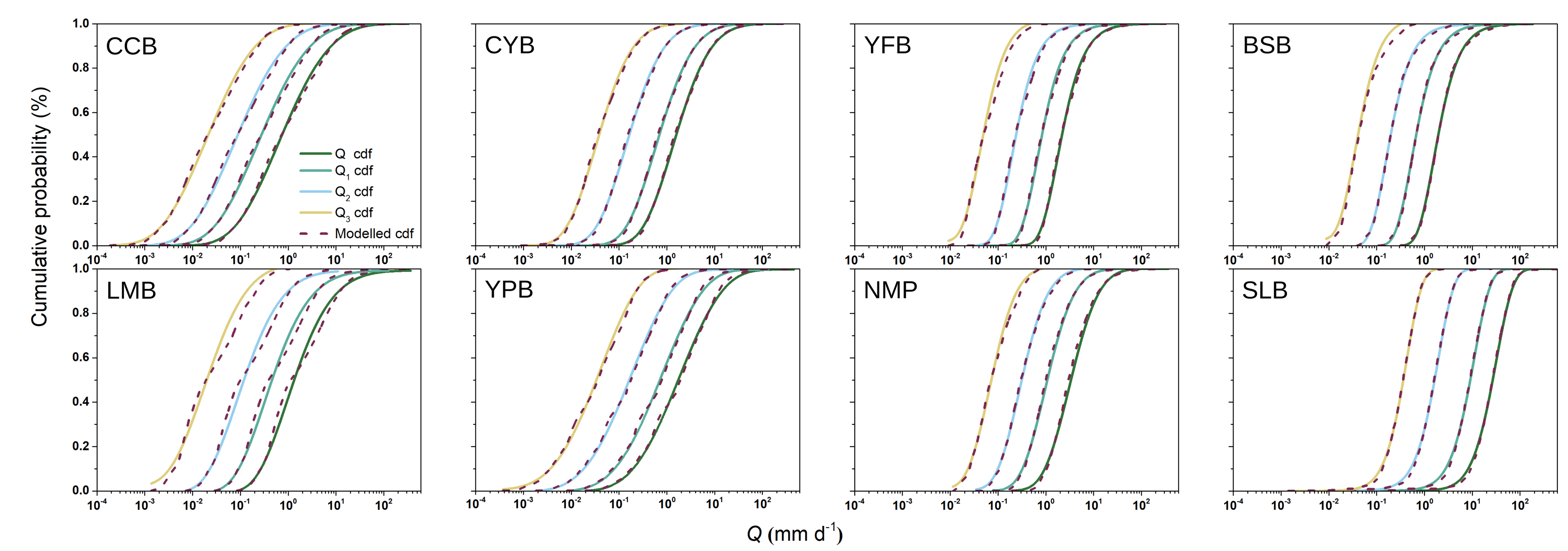

Fig. 5 FDCs corresponding to different Q_i and modelled results in each catchment .

Table. 3 Kolmogorov-Smirnov distance (c^{KS}) of different streamflow structures in each catchment

$c^{KS}(Q_i)$	CCB	CYB	YFB	BSB	LMB	YPB	NMP	SLB
$c^{KS}(Q)$	0.032	0.030	0.032	0.019	0.075	0.036	0.054	0.026
$c^{KS}(Q_1)$	0.032	0.030	0.035	0.018	0.076	0.039	0.038	0.026
$c^{KS}(Q_2)$	0.033	0.029	0.042	0.017	0.079	0.038	0.025	0.026
$c^{KS}(Q_3)$	0.036	0.027	0.072	0.054	0.098	0.039	0.050	0.021

5.3 Recession parameter (a and b)

- As the flow component structure becomes slower, most catchment exhibit a decrease in parameters a and b, with the change in b being relatively slight.

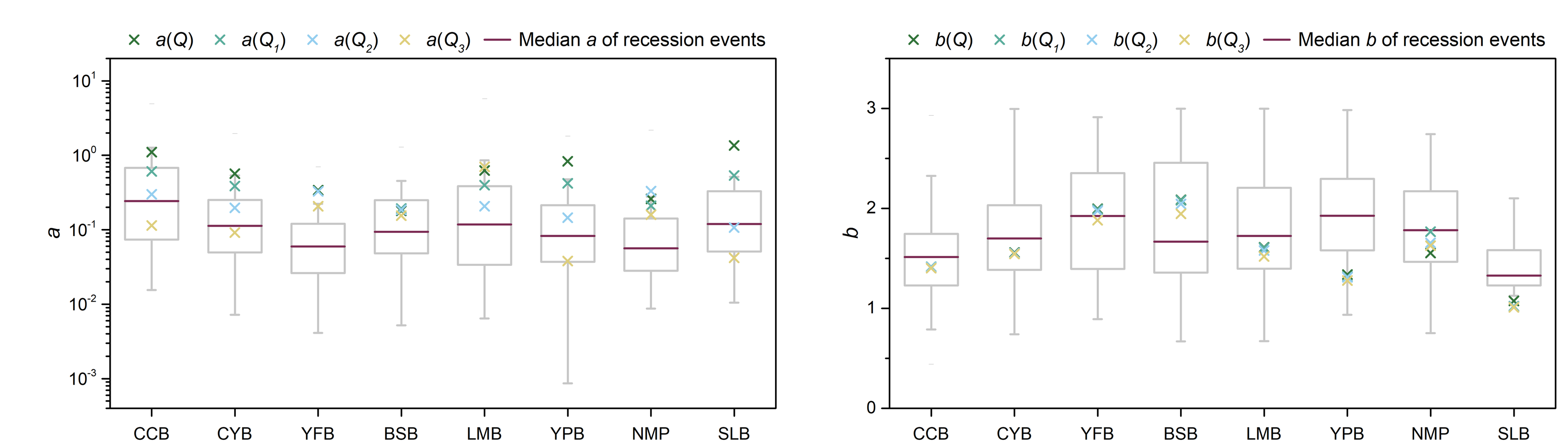

Fig. 6 Parameter a and b corresponding to different Q_i in each catchment